

**AFRL-DE-PS-
TP-2006-1011**

**AFRL-DE-PS-
TP-2006-1011**

Studies of a Mesospheric Sodium Guidestar Pumped by Continuous Wave Sum-Frequency Mixing of Two Nd: YAG Laser Lines in Lithium Triborate (Preprint)

John Telle, et al.

16 May 06

Conference Paper

APPROVED FOR PUBLIC RELEASE; DISTRIBUTION IS UNLIMITED.

This material is declared a work of the US Government and is not subject to copyright protection in the United States.



**AIR FORCE RESEARCH LABORATORY
Directed Energy Directorate
3550 Aberdeen Ave SE
AIR FORCE MATERIEL COMMAND
KIRTLAND AIR FORCE BASE, NM 87117-5776**

REPORT DOCUMENTATION PAGE

*Form Approved
OMB No. 0704-0188*

Public reporting burden for this collection of information is estimated to average 1 hour per response, including the time for reviewing instructions, searching existing data sources, gathering and maintaining the data needed, and completing and reviewing this collection of information. Send comments regarding this burden estimate or any other aspect of this collection of information, including suggestions for reducing this burden to Department of Defense, Washington Headquarters Services, Directorate for Information Operations and Reports (0704-0188), 1215 Jefferson Davis Highway, Suite 1204, Arlington, VA 22202-4302. Respondents should be aware that notwithstanding any other provision of law, no person shall be subject to any penalty for failing to comply with a collection of information if it does not display a currently valid OMB control number. PLEASE DO NOT RETURN YOUR FORM TO THE ABOVE ADDRESS.

1. REPORT DATE (DD-MM-YYYY) 16 May 2006		2. REPORT TYPE Conference Paper Preprint		3. DATES COVERED (From - To) 1 Oct 02 - 30 Apr 06	
4. TITLE AND SUBTITLE Studies by a Mesospheric Sodium Guidestar Pumped by Continuous Wave Sum-Frequency Mixing of Two Nd: YAG Laser in Lithium Triborate (Postprint)				5a. CONTRACT NUMBER DF 297062 (In-House)	
				5b. GRANT NUMBER	
				5c. PROGRAM ELEMENT NUMBER 63605F	
				5d. PROJECT NUMBER 5076	
				5e. TASK NUMBER SA	
				5f. WORK UNIT NUMBER 01	
7. PERFORMING ORGANIZATION NAME(S) AND ADDRESS(ES) AFRL/DES 3550 Aberdeen Avenue SE Kirtland AFB, NM 87117-5776				8. PERFORMING ORGANIZATION REPORT NUMBER	
				10. SPONSOR/MONITOR'S ACRONYM(S)	
9. SPONSORING / MONITORING AGENCY NAME(S) AND ADDRESS(ES) Air Force Research Laboratory New Mexico Institute of Mining 3550 Aberdeen Avenue SE And Technology Kirtland AFB, NM 87117-5776 801 Leroy Place Socorro, NM 87801				11. SPONSOR/MONITOR'S REPORT NUMBER(S) AFRL-DE-PS-TP-2006-1011	
12. DISTRIBUTION / AVAILABILITY STATEMENT Approved for Public Release; Distribution is Unlimited.					
13. SUPPLEMENTARY NOTES Submitted for presentation at SPIE Defense & Security Symposium, Conference 6215, Orlando, FL, 17-21 April 2006. This material is declared a work of the US Government and is not subject to copyright protection in the United States.					
14. ABSTRACT Mesospheric sodium guidestar radiance is plotted vs. wavelength, fason power, fason polarization and date. Peak radiance for circular polarization was about 7000 photons/sec/cm ² (V1 magnitude = 5.1) for 30 watts of pump power in November of 2005. Pumping with circular polarization at high power produces about 2 times more return than linear polarization. Pumping D2a at high power produces about 12 times more return than pumping D2b. A lidar equation is used to determine column density. Estimated maximum possible guidestar radiance is about 3 times greater than measured values. Guidestar radiance may be saturated by atoms becoming trapped in F' = 1 and atomic recoil.					
15. SUBJECT TERMS Sodium guidestar, adaptive optics, sum-frequency mixing, lithium triborate, Nd:YAG					
16. SECURITY CLASSIFICATION OF:			17. LIMITATION OF ABSTRACT SAR	18. NUMBER OF PAGES 11	19a. NAME OF RESPONSIBLE PERSON John Telle
a. REPORT Unclassified	b. ABSTRACT Unclassified	c. THIS PAGE Unclassified			19b. TELEPHONE NUMBER (Include area code)

CLEARED
FOR PUBLIC RELEASE
AFRL/ODE-PA
22 MAR 06

Studies of a Mesospheric Sodium Guidestar Pumped by Continuous-Wave Sum-Frequency Mixing of Two Nd:YAG Laser Lines in Lithium Triborate

John Telle^a, Jack Drummond^a, Craig Denman^a, Paul Hillman^a, Gerald Moore^a, Steven Novotny^a, Robert Fugate^b

^aStarfire Optical Range, Air Force Research Laboratory, 3550 Aberdeen Ave. SE, Kirtland AFB, NM 87117-5776

^bNew Mexico Institute of Mining and Technology, 801 Leroy Place, Socorro, NM 87801

ABSTRACT

Mesospheric sodium guidestar radiance is plotted vs. wavelength, laser power, laser polarization and date. Peak radiance for circular polarization was about 7000 photons/sec/cm² (V_1 magnitude = 5.1) for 30 watts of pump power in November of 2005. Pumping with circular polarization at high power produces about 2 times the return as linear polarization. Pumping D_{2a} at high power produces about 12 times the return as pumping D_{2b}. A lidar equation is used to determine column density. Estimated maximum guidestar radiance is about 3 times greater than measured values. Guidestar radiance may be saturated by atoms being trapped in F'=1 and atomic recoil.

Keywords: Sodium Guidestar, Adaptive Optics, Sum-Frequency Mixing, Lithium Triborate, Nd:YAG

1. INTRODUCTION

Adaptive Optics is capable of significantly improving the resolution of ground-based telescopes¹. Mesospheric sodium guidestars² result in lower focus anisoplanatism due to their greater altitude (~ 92 km). Multiconjugate adaptive optics uses more than one guidestar and deformable mirror to further reduce anisoplanatism. A sodium guidestar is typically produced by laser excitation of a tenuous layer of sodium atoms persisting after ablation from incoming meteors. The required guidestar size ranges from ~1-2 arcseconds (~45-90 cm) and radiance at the telescope primary mirror from ~150 to 4000 photons/cm²/sec depending on the application (e.g. astronomy or satellite imaging) and the site.

2. GUIDESTAR PUMP FASOR

At the Starfire Optical Range we are pursuing a sodium guidestar pumped by a narrow-linewidth, continuous-wave frequency addition source of optical radiation (FASOR) at 589 nm. The source is continuously tunable across the entire sodium D₂ line and is capable of pumping either the D_{2a} or D_{2b} feature with linear or circular polarization. We have built two FASORS, a 20-watt table-top version,^{3,4} and a 50-watt automated version^{5,6} which has been mounted on the 3.5-meter telescope at the site. The 589 nm is produced by resonant sum-frequency mixing of the 1064-nm and 1319-nm Nd:YAG laser lines in a bow-tie-shaped cavity. Non-planar ring oscillators provide the wavelength stability and injection-locked power oscillators the power. The sum-frequency generator is resonant at both Nd:YAG laser lines, uses antireflection coated lithium triborate (LBO) and has reached 60 % conversion efficiency.

3. SKY TESTING RESULTS AND GUIDESTAR PROPERTIES

Figure 1 shows the results of 8 scans of guidestar radiance vs. pump laser wavelength in August, October, November and December of 2005. The guidestar radiance is for pumping with circular polarization and is given in photons/sec/cm² and the wavelength is given in nanometers. We believe the laser at launch is about 80% circularly polarized but the polarization has not been measured at the output of the launch optics. The radiance in photons/sec/cm² is at the "top of the telescope" or the value after attenuation by the atmosphere. Also shown in the figure is the laser

AFRL/ODE 06-104

power out the laser box and the V_1 magnitude of the guidestar at the peak of the radiance curve. V_1 is the V magnitude of the guidestar "above the atmosphere" (before atmospheric attenuation) corrected for the transmission of a normalized astronomical V filter with a fwhm of 78.5 nm mounted in front of the radiometry camera.¹¹ The laser power out the laser box will be attenuated by the launch optics and atmosphere before reaching the sodium layer. Our maximum return to date was about 7000 photons/sec/cm² obtained on November 16, 2005. Note that value was obtained with 30 watts of laser power whereas the maximum laser power shown for these data was 40 watts. We believe the variation in maximum return is due mostly to variations in column density. The 50-watt automated laser was used for the work described in this paper.

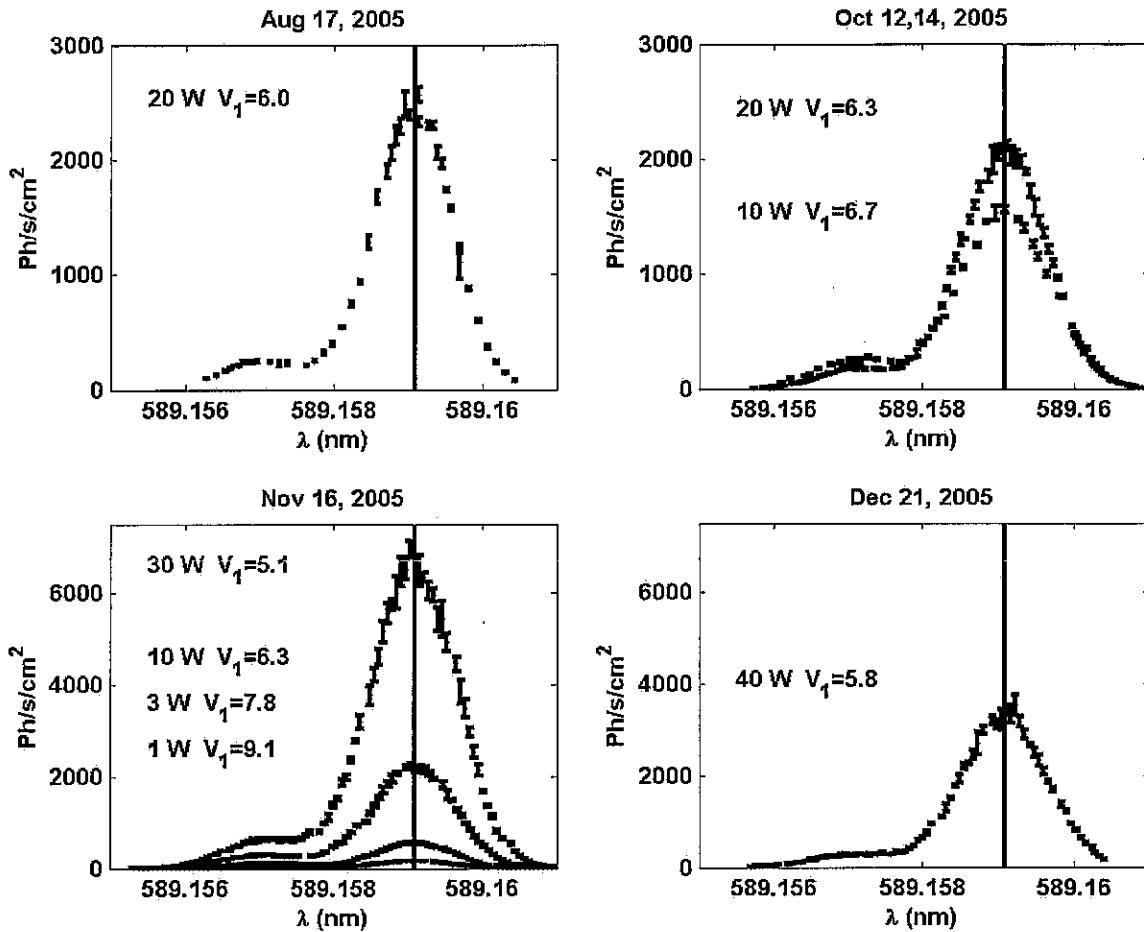


Figure 1. Guidestar radiance in photons/sec/cm² vs. laser wavelength for 5 nights in the Fall of 2005. Also shown is the guidestar V_1 magnitude corresponding to the peak radiance and the laser power for the run. These results are for pumping with circular polarization using the 50-watt laser.

Figure 2 shows the same results as those shown in figure 1 except the laser polarization is linear. We believe the laser at launch was about 100 % linearly polarized but it has not been measured.

Figure 3 uses the results from figures 1 and 2. The upper plot gives the peak guidestar radiance when pumping D_{2a} divided by the peak guidestar radiance when pumping D_{2b} vs. laser power for both linear and circular laser polarization. The ratios are fit to the function $a \ln(1 + (P_L/b)) + 5/3$. The 5/3 is chosen from theory; this should be the ratio of the guidestar radiance while pumping with low power where the atomic energy levels remain in thermal equilibrium. The

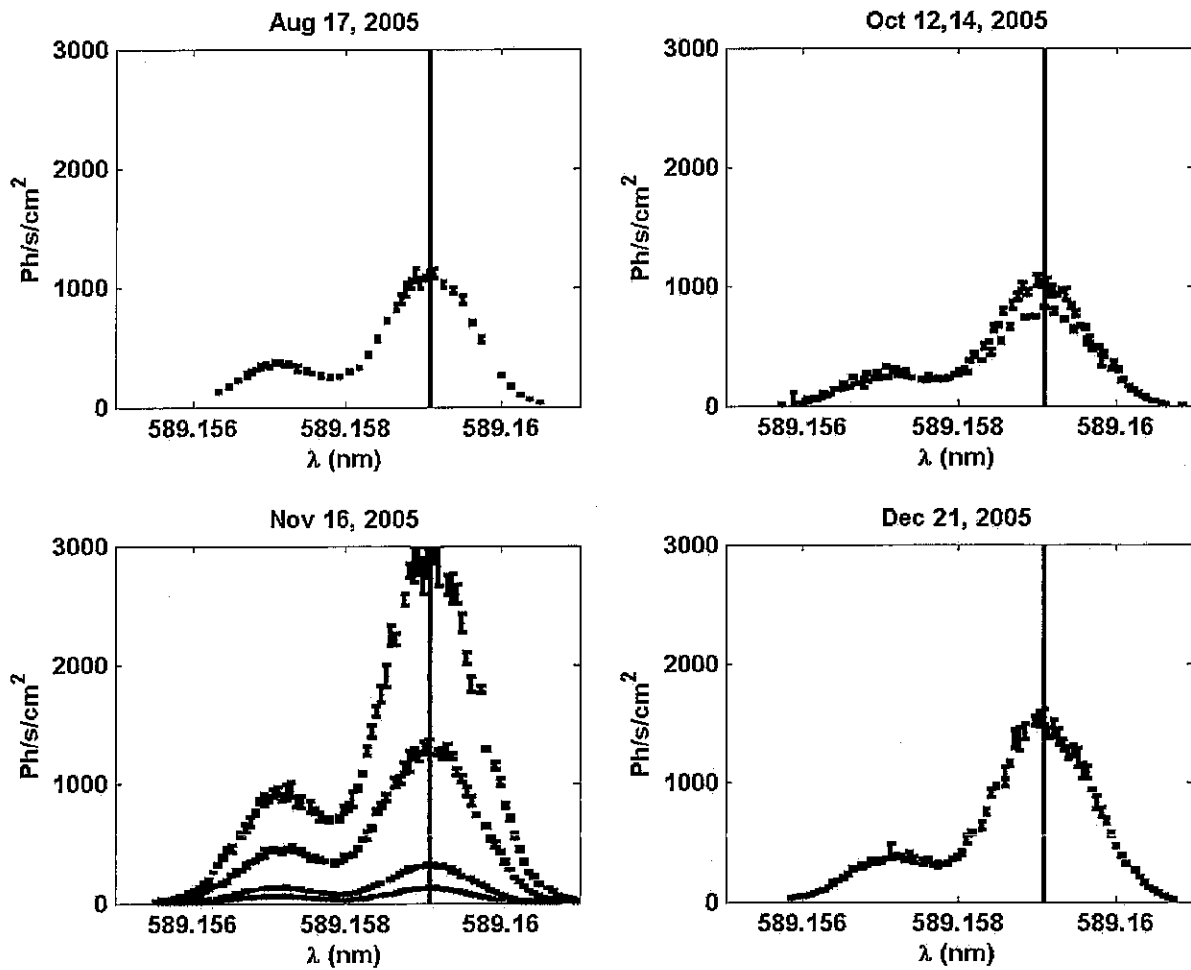


Figure 2. The conditions are the same as figure 1 except the laser polarization is linear.

plot shows pumping D₂a is much more (about 12 times) effective than pumping D₂b for circular polarization. However for linear polarization pumping D₂a is only about 3 times more effective than pumping D₂b.

The lower plot of figure 3 shows the guidestar radiance when pumping with circular polarization divided by the guidestar radiance when pumping with linear polarization for both D₂a and D₂b. The ratio is fit to the function $a \ln(1 + (P_L/b)) + 1$. The 1 is chosen because at low power, pumping with circular polarization should give the same result as pumping with linear polarization. The plot shows pumping D₂a with circular polarization is about 2 times more effective at high power than pumping with linear polarization. However pumping D₂b with circular polarization is less effective than pumping with linear polarization at high power.

Figure 4 shows the guidestar radiance vs. pump laser power for circular and linear polarization on December 22, 2005. For these results the laser is tuned to the peak of D₂a. The reduced maximum return relative to December 21 is probably due to a column density variation. The upper plot fits the data to $R = a \ln(1 + (P_L/P_{sat}))$ where \ln represents the natural logarithm function. The lower plot fits the data to $R = a \operatorname{atanh}(P_L/P_{sat}) + b P_L$ where \tanh represents the hyperbolic tangent function. We also tried fitting the data to a linear function ($R = a P_L$). The logarithm function was motivated by the result that a homogeneously broadened line pumped by a Gaussian spatial distribution results in a

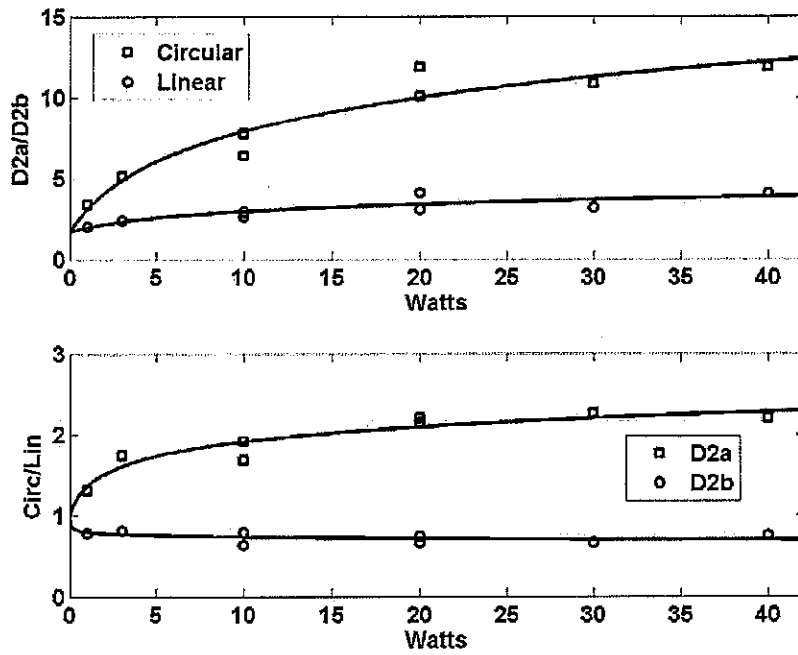


Figure 3. Upper plot is the ratio of peak guidestar radiance while pumping D2a divided by the peak guidestar radiance while pumping D2b vs. laser power for circular and linear laser polarization. Lower plot is the peak guidestar radiance while pumping with circular polarization divided by the peak guidestar radiance while pumping with linear polarization vs. laser power for pumping D2a and D2b.

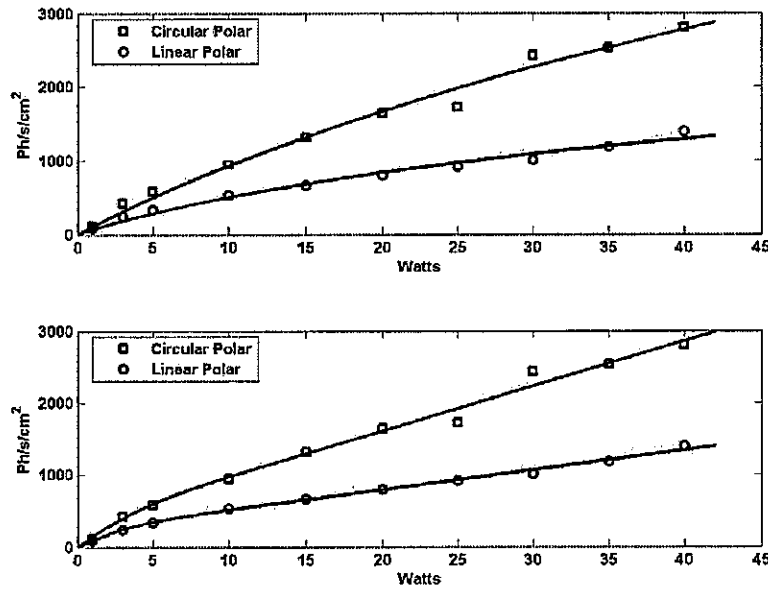


Figure 4. Guidestar radiance vs. laser power on December 22, 2005 for circular and linear laser polarization. For these results the laser is tuned to the peak of D2a.

natural logarithm response. However the atomic sodium line in the mesosphere is inhomogeneously broadened with about a 1 GHz Doppler width and the laser spectral distribution is small compared to the sodium natural linewidth of 10 MHz. The tanh plus linear function was motivated by the expectation that at relatively low power the circular polarization result should be concave up due to optical pumping later rolling over to concave down due to saturation. The data fit fairly well to these functions but not much data was taken at low power due to signal to noise problems. Our goal is to use the fits to determine the slope of the guidestar radiance vs. laser power at zero power. This is related to the column density of the sodium in the mesosphere (see section 4). Another way to simulate low power in the mesosphere is to increase the spot size since low intensity is actually what is needed to reach the small signal regime. We hope to try this in the future.

Note that the response for linear polarization saturates more quickly than the response for circular polarization. We believe this is due to atoms decaying into $F'=1$ which shifts their absorption peak off the laser line by 1.772 GHz. This causes them to become trapped in $F'=1$. Circular polarization tends to trap atoms in the optically pumped pair of states which forbids decay into $F'=1$ by atomic selection rules. This pair of states gives rise to greater guidestar radiance (see section 4).

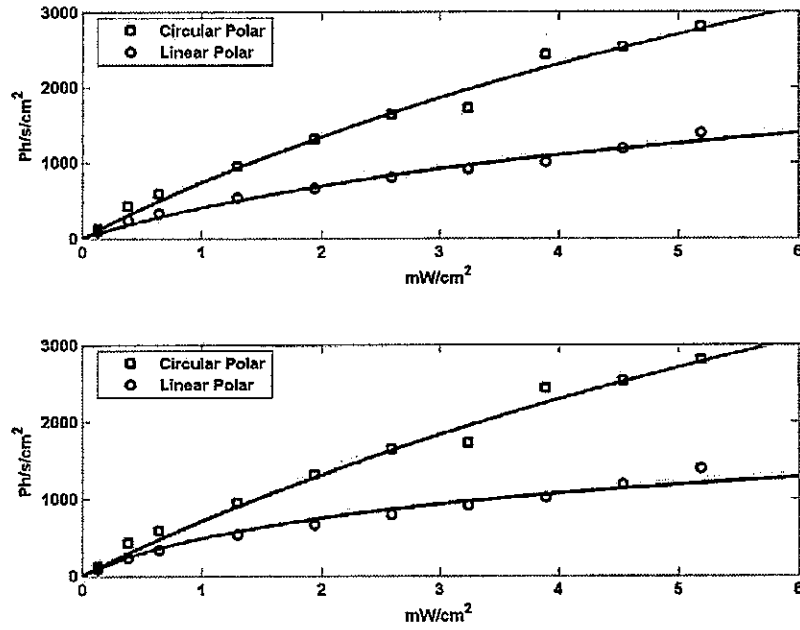


Figure 5. Guidestar radiance vs. laser intensity in the mesosphere where the intensity is produced from a spot fwhm determined from multiframe blind deconvolution of images.

We also attempted to determine guidestar size in the mesosphere from multi-frame blind deconvolution of images taken with the laser tuned to the peak of D_2a . We saw no obvious correlation of image size with laser power. The average fwhm for December 22, 2005 was $75.6 \text{ cm} \pm 2.3 \text{ cm}$. Using this value the laser power was converted to intensity by dividing by $\pi \text{ fwhm}^2/4 \ln 2$. This produces the peak intensity of a Gaussian beam ($I = (2 P_L/\pi w^2) \exp(-2r^2/w^2)$) with a spot radius $w = 0.85 \times \text{fwhm}$, or a “top-hat” (uniform intensity profile) beam with a diameter equal to $(\sqrt{2}) \times w$. This operation converts figure 4 into figure 5.

The upper data was fit to the function $R = a \ln(1 + I_L/I_{sat})$. The slope at zero laser intensity was equal to 815 ± 270 photons/sec/mW (490 ± 65 photons/sec/mW) for circular (linear) pump laser polarization. Thus the slopes at zero intensity are not equal. We attribute this to insufficient data at low power. The saturation intensity was $4.2 \pm 1.7 \text{ mW/cm}^2$ ($2.1 \pm 0.7 \text{ mW/cm}^2$) for circular (linear) pump laser polarization. The theoretical saturation intensity for the

optically pumped pair of states is 6.4 mW/cm^2 . Optical pumping only occurs for circular polarization. For a thermal distribution of atomic states the saturation intensity is about $10\text{-}20 \text{ mW/cm}^2$. Thus the low saturation intensities with the value for linear polarization being even lower than the value for circular polarization indicates some other process than saturation of optical absorption is involved. Again we feel this may be trapping in $F'=1$.

Figure 6 gives an indication of the column density variation throughout the year with data was taken in November of 2002, March and July of 2003, and August through December of 2005. The slopes at zero power are plotted for circular and linear polarization and again they should be equal. The plot indicates we can expect about a factor of 2 increase in column density in November compared to July.

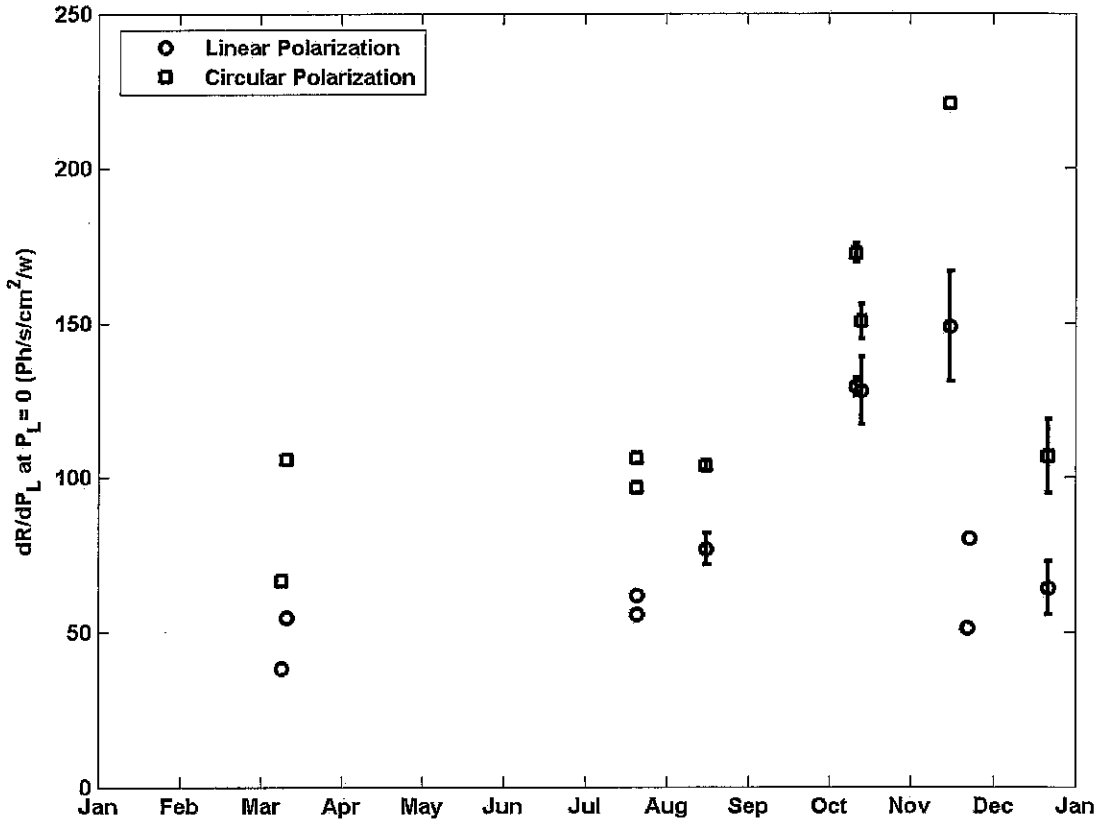


Figure 6 Slope of guidestar radiance vs. laser power at zero power, vs. month of the year and pump laser polarization. This is an indication of the sodium column density variation throughout the year.

4. COMPARING ESTIMATES OF MAXIMUM GUIDESTAR RADIANCE WITH MEASURED VALUES

In this section we compare the maximum achievable guidestar radiance per watt of pump laser power from a theoretical estimate with the measured value. Our ultimate goal is to determine how we might modify the laser to approach this maximum. Milonni et. al.⁷ have estimated analytically the radiance from a column of unsaturated optically-pumped atoms. This means that all the atoms reside in two ($F=3, M=3$; and $F'=2, M'=2$) of the 24 states (16 upper and 8 ground states) normally contributing to the sodium D₂ line and almost all the atoms reside in the lower state of the pair. This pair of states has a fluorescence pattern enhanced in the direction towards the pump laser and the largest absorption

cross section. This situation should correspond to the greatest radiance per watt of pump laser power back towards the telescope. For a column density of 3.7×10^9 atoms/cm² and an atmospheric transmission of 1 they obtain 330 photons/cm²/sec/watt. Operationally to achieve the theoretical maximum it will be necessary to optically pump all the atoms to this pair of states without saturating the optical transition, or trapping atoms in other states or velocity classes which are not pumped. Before reaching the optically pumped condition atoms can fluoresce into F'=1 which is out of resonance with the pump laser frequency by 1.772 GHz. Atoms move out of the velocity class which is pumped through atomic recoil. Collisions are constantly thermalizing F'=2 and F'=1, working against optical pumping and trapping. Velocity changing collisions are constantly thermalizing the atomic velocity distribution working against atomic recoil.

In order to calculate the return from this pair of states we will need the mesospheric atomic column density (ρ in atoms/cm²) which corresponds to the measured guidestar radiance (R in photons/sec/cm²) at the corresponding laser power (P_L in watts). The column density is calculated by integrating the local atomic density [atoms/cm³] through the mesosphere.

To determine ρ we will use the slope of guidestar radiance vs. laser power ($\Delta R/\Delta P_L$) at low laser power. By using the slope of measured guidestar radiance vs. pump laser power at low power we hope to obtain radiance based on the small-signal thermal-equilibrium atomic cross section which has been calculated^{8,9} (1×10^{-11} cm²). At low power the atoms remain in thermal equilibrium whereas at higher powers they become optically pumped and this changes the absorption cross section. We will also use lidar equation 28 of Gardner.¹⁰ We integrate both sides of the equation through the mesosphere and obtain the total guidestar radiance due to column density ρ . We normalize with respect to integration time, detection efficiency and telescope primary mirror area. Equation 1 gives the column density in terms of the limit at low power of the slope of R vs. P_L .

$$\rho = \underset{P_L \rightarrow 0}{\text{Limit}} \frac{\Delta R}{\Delta P_L} \times \frac{hc}{\lambda} \times \frac{4\pi z^2}{T_A^2 \sigma} \quad (1)$$

In equation (1) σ is the atomic cross section, z is the range to the mesospheric sodium, λ is the wavelength of the pump laser (~589 nm), and T_A is the atmospheric transmission. We assume z is constant for the integral through the mesospheric sodium layer (z is approximately 92 km whereas the layer thickness is about 6 km).

Table 1 gives the slope of guidestar radiance vs. laser power at low power from fit functions. For the October data a natural logarithm function plus a constant was used for both circular and linear polarization. For November a linear function was used for circular polarization, and natural logarithm function plus a constant for the linear polarization. For the December data we used a tanh plus a linear function for circular polarization and a natural logarithm plus a linear function for linear polarization and forced the two slopes at low power to be the same. As the table shows the slopes at low power are not equal except for December. We attribute this to insufficient data at low intensity, the small signal regime. Atomic sodium has such a large cross section it does not take much laser intensity to push the distribution to non-thermal. To calculate the column density we will use the average of the two values.

Sky Test Date	Slope of guidestar radiance vs. laser power at low power [photons/cm ² /sec/watt]		
	Circular Polarization	Linear Polarization	Average
12 October 2005	170	130	150
14 October 2005	150	130	140
16 November 2005	220	150	185
22 December 2005	143	143	143

Table 1. Slope of guidestar radiance vs. laser power at low power for circular and linear polarization and a representative sample of sky tests in October, November, and December. The slopes are determined from functions fit to the measurements as described in the text.

Using equation 1, the average values in Table 1 for the slope of guidestar radiance vs. laser power at low power, and the constants given above we obtain Table 2 for column density corresponding to the guidestar radiance curves on the respective dates.

Date	T_A	Average slope of guidestar radiance vs. laser power at low power [photons/cm ² /sec/watt]	Calculated column density, ρ , from equation (1) [atoms/cm ²]
12 October 2005	0.85	150	7.5×10^9
14 October 2005	0.85	140	7.0×10^9
16 November 2005	0.89	185	8.4×10^9
22 December 2005	0.84	143	7.3×10^9

Table 2. Calculated column density from equation 1 and the low-power slope of guidestar radiance vs. laser power.

Milonni et. al.⁷ have also estimated from theory the guidestar radiance per watt of laser power in the small-signal thermal-equilibrium regime. Assuming unity atmospheric transmission and a column density of 3.7×10^9 atoms/cm² they obtain 110 photons/cm²/sec/watt. We scale this result using our calculated column density and the appropriate atmospheric transmission to obtain Table 2 which compares the estimated guidestar radiance per watt of laser power in the small-signal regime with the measured value.

Date	Theoretical estimate of the slope of guidestar radiance vs. laser power [photons/cm ² /sec/watt]	Calculated slope of the guidestar radiance vs. laser power from measurements [photons/cm ² /sec/watt]
12 October 2005	161	150
14 October 2005	150	140
16 November 2005	198	185
22 December 2005	153	143

Table 3. Comparison of the theoretical estimate of the small-signal thermal-equilibrium slope of guidestar radiance vs. laser power with the value calculated from functions fit to the measurements.

The reasonable agreement between the theoretical estimate and the value from functions fit to the data suggests our column density estimates are acceptable. We use these estimates to scale the theoretical estimate of Milonni et. al.⁷ for the maximum slope of guidestar radiance vs. laser power and compare this with our calculated values from functions fit to the data. In this case however we compare to the slope of the fit functions for circular polarization rather than the average of the results for circular and linear polarization. We do this because the circular polarization results had greater slope probably due to some degree of optical pumping. The maximum possible slope was given in the first paragraph of this section. Table 4 makes this comparison.

We feel the two most probable reasons our measured guidestar radiance is about 3 times less than the maximum possible radiance are: (1) atoms are becoming trapped in $F' = 1$ (the energy level associated with the D₂b absorption) where the pumping rate is very slow with the laser tuned to pump $F'=2$ (D₂a absorption), and (2) atoms are recoiling off the pump laser line into velocity classes which are weakly pumped. Other possibilities are laser beam power and polarization changes due to the launch optics.

Date	Calculated slope of guidestar radiance vs. laser power from measurements with circular polarization pumping [photons/cm ² /sec/watt]	Theoretical estimates of the maximum slope of guidestar radiance vs. laser power [photons/cm ² /sec/watt]	Ratio of the maximum slope to one based on measurements for circular polarization
12 October 2005	170	483	2.8
14 October 2005	150	451	3.0
16 November 2005	220	593	2.7
22 December 2005	143	459	3.2

Table 4. Comparison of the calculated slope of guidestar radiance vs. laser power at low power from functions fit to measurements with theoretical estimates of the maximum slope of guidestar radiance vs. laser power.

REFERENCES

1. Michael Roggemann, Byron Welsh, Robert Fugate, "Improving the resolution of ground-based telescopes," *Reviews of Modern Physics*, Vol. 69, pgs. 437-505, 1997.
2. W. Happer, G. MacDonald, C. Max, F. Dyson, "Atmospheric-turbulence compensation by resonant optical backscattering from the sodium layer in the upper atmosphere," *Jour. Opt. Soc. Am. A*, Vol. 11, pgs. 263-276, 1994.
3. Joshua Bienfang, Craig Denman, Brent Grime, Paul Hillman, Gerald Moore, John Telle, "20 Watt CW All-Solid-State 589-nm Sodium Beacon Excitation Source Based on Doubly Resonant Sum-Frequency Generation in LBO," *Trends in Optics and Photonics, Advanced Solid-State Photonics*, Vol. 83, pgs. 111-120, 2003.
4. Craig Denman, Paul Hillman, Gerald Moore, John Telle, Jack Drummond, Andrea Tuffli, "20 W CW 589 nm sodium beacon excitation source for adaptive optical telescope applications," *Optical Materials*, Vol. 26, pgs. 507-513, 2004.
5. Craig Denman, Paul Hillman, Gerald Moore, John Telle, "Realization of a 50-watt facility-class sodium guidestar pump laser," *Proceedings of the SPIE*, Vol. 5707, pgs. 46-49, 2005.
6. Robert Fugate, Craig Denman, Paul Hillman, Gerald Moore, John Telle, Imelda De La Rue, Jack Drummond, James Spinhirne, "Progress toward a 50-watt facility-class sodium guidestar pump laser," *Proceedings of the SPIE*, Vol. 5490, pgs. 1010-1020, 2004.
7. Peter Milonni, Heidi Fearn, John Telle, Robert Fugate, "Theory of continuous-wave excitation of the sodium beacon," *Jour. Opt. Soc. Am. A*, Vol. 16, pgs. 2555-2566, 1999.
8. Peter Milonni, Robert Fugate, John Telle, "Analysis of measured photon returns from sodium beacons," *Jour. Opt. Soc. Am. A*, Vol. 15, pgs. 217-233, 1998.
9. J. R. Morris, "Efficient excitation of a mesospheric sodium laser guide star by intermediate duration pulses," *Jour. Opt. Soc. Am. A*, Vol. 11, pgs. 832-845, 1994.
10. Chester Gardner, "Performance capabilities of middle-atmosphere temperature lidars: comparison of Na, Fe, K, Ca, Ca⁺, and Rayleigh Systems," *Applied Optics*, Vol. 43, pgs. 4941-4956, 2004.
11. Jack Drummond, John Telle, Craig Denman, Paul Hillman, Jim Spinhirne, and Julian Christou, "Photometry of a Sodium Laser Guidestar from the Starfire Optical Range. II. Compensating the Pump Beam," *Publications of the Astronomical Society of the Pacific*, Vol. 116, pgs. 952-964, 2004.